

Projector self-consistent DFT+ U using non-orthogonal generalized Wannier functions

David D. O'Regan,^{1,*} Nicholas D. M. Hine,^{1,2} Mike C. Payne,¹ and Arash A. Mostofi²

¹*Cavendish Laboratory, University of Cambridge,
J. J. Thomson Avenue, Cambridge CB3 0HE, United Kingdom*

²*The Thomas Young Centre, Imperial College London, London SW7 2AZ, United Kingdom*
(Dated: November 2, 2018)

We present a formulation of the density-functional theory + Hubbard model (DFT+ U) method that is self-consistent over the choice of Hubbard projectors used to define the correlated subspaces. In order to overcome the arbitrariness in this choice, we propose the use of non-orthogonal generalized Wannier functions (NGWFs) as projectors for the DFT+ U correction. We iteratively refine these NGWF projectors and, hence, the DFT+ U functional, such that the correlated subspaces are fully self-consistent with the DFT+ U ground-state. We discuss the convergence characteristics of this algorithm and compare ground-state properties thus computed with those calculated using hydrogenic projectors. Our approach is implemented within, but not restricted to, a linear-scaling DFT framework, opening the path to DFT+ U calculations on systems of unprecedented size.

PACS numbers: 71.15.Mb, 31.15.E-, 71.15.Ap (Accepted for Physical Review B Rapid Communications)

The physics of localized electrons bound to transition metal or Lanthanoid ions is important for understanding and harnessing the behaviour of complex systems such as molecular magnets¹ inorganic catalysts² and the organometallic molecules that facilitate some of the most critical chemical reactions in biochemistry³.

Despite its success at predicting ground-state properties of materials, Kohn-Sham density-functional theory (DFT)⁴ fails to describe the physics of such “correlated-electron” systems when local or semi-local exchange-correlation (XC) functionals are used, often predicting results that are not only quantitatively but qualitatively inconsistent with experiment⁵. The origin of this apparent failure has been understood since the work of Perdew *et al.*⁶ and is related to the unphysical curvature of the energy functional with respect to electronic occupation number^{7,8} inherent to such functionals unless a self-interaction correction is employed⁹.

DFT + Hubbard U (DFT+ U)¹⁰ is a simple, computationally inexpensive method for improving the description of on-site Coulomb interactions provided by conventional XC functionals and, hence, for extending the range of applicability of DFT to strongly-correlated materials.

The principle of DFT+ U is to divide the system into a delocalized, free electron-like part, the “bath”, which is well-described by conventional XC functionals, and a set of “correlated sites” which is not. The XC functional for electrons associated with these sites is then explicitly augmented with screened Coulomb interactions, the form of which are inspired by the Hubbard-model¹¹, together with a double-counting term to correct for the component already included within the XC functional.

The correlated sites are defined by a set of $3d$ and/or $4f$ atomic-like orbitals, or “Hubbard projectors”, that are chosen *a priori*. Projector functions that are commonly used include hydrogenic wavefunctions⁷, maximally-localized Wannier functions¹², and LMTO-type orbitals^{5,10}. This arbitrariness constitutes an unsatisfactory, adjustable parameter in the DFT+ U method.

In this article, we present an approach in which the ambiguity in the choice of Hubbard projectors is removed, and in which they are determined self-consistently with respect to the DFT+ U ground-state. We first outline the theoretical framework of our approach, and present results of calculations on ligated iron porphyrin. We examine the adequacy of hydrogenic orbitals as Hubbard projectors and, in particular, the sensitivity of the results to the form of these orbitals. We show that optimized non-orthogonal generalized Wannier functions (NGWFs) provide an unambiguous and natural choice for Hubbard projectors and we introduce a technique for self-consistently delineating the subspaces in which correlation effects play an important role.

Our implementation is within the framework of linear-scaling DFT, however, the same self-consistent projector methodology may be applied to any DFT approach that solves for localized Wannier-like functions (either directly, or indirectly in a post-processing step using an interface to a code such as Wannier90¹³). Furthermore, our approach may be readily combined with recently-proposed methods to calculate U parameters from first-principles^{7,14}, facilitating entirely parameter-free and self-consistent DFT+ U calculations.

The Hubbard energy correction term in DFT+ U can be interpreted as a functional that penalizes the unphysical non-integer occupancy of the spatially localized d - or f -orbitals, those that are most prone to the spurious self-interaction present in standard DFT XC functionals.

We use a rotationally-invariant correction term,

$$E_U = \sum_{I\sigma} \frac{U^{(I)(\sigma)}}{2} \left[\sum_m n_m^m - \sum_{mm'} n_m^{m'} n_{m'}^m \right]^{(I)(\sigma)}, \quad (1)$$

where $U^{(I)(\sigma)}$ represents the screened Coulomb repulsion between electrons of spin σ , localized on the correlated site I . Eq. (1) is, in effect, a penalty functional for deviation from idempotency of the projection of the single-particle density-matrix onto each correlated subspace.

The occupancy matrix in the case of a set of M *non-orthogonal* Hubbard projectors $|\varphi_m^{(I)}\rangle$, $m \in \{1, \dots, M\}$, localized on site I , is given by

$$n_m^{(I)(\sigma)m'} = \sum_{i\mathbf{k}} f_{i\mathbf{k}}^{(\sigma)} \langle \psi_{i\mathbf{k}}^{(\sigma)} | \hat{P}_m^{(I)m'} | \psi_{i\mathbf{k}}^{(\sigma)} \rangle, \quad (2)$$

where $\psi_{i\mathbf{k}}^{(\sigma)}$ is a Kohn-Sham eigenstate for spin channel σ with band index i , crystal momentum \mathbf{k} and occupancy $f_{i\mathbf{k}}^{(\sigma)}$, and $\hat{P}_m^{(I)m'} = |\varphi_m^{(I)}\rangle \langle \varphi_{m'}^{(I)m'}|$ is the Hubbard projection operator. The contravariant dual vectors $|\varphi^{(I)m}\rangle$ are related to the covariant projectors through the site-centered overlap matrix $O_{mm'}^{(I)} = \langle \varphi_m^{(I)} | \varphi_{m'}^{(I)} \rangle$ which is a metric on the correlated subspace $\mathcal{C}^{(I)}$: $|\varphi^{(I)m}\rangle = |\varphi_{m'}^{(I)}\rangle O_{m'm}^{(I)}$; $O_{m'm''}^{(I)} O_{m''m}^{(I)} = \delta_m^{m'}$.

Our definition of the occupancy matrix differs to that of Refs. 15 and has the following desirable properties: the expressions are tensorially correct; the energy and resulting potential are rotationally invariant; the resulting potential is Hermitian and localized to the correlated site; and the trace of the occupancy matrix gives the occupancy of the correlated site¹⁶. The contravariant metric $O^{(I)mm'}$ is calculated only as an inverse of the covariant overlap matrix $O_{mm'}^{(I)}$, therefore, the duals of the Hubbard projectors are also localized to the site. As a result, and in contrast with previously proposed approaches to DFT+ U models using non-orthogonal projectors, the DFT+ U potential constructed from the tensorially consistent energy for a given correlated site remains manifestly local to that site. We note that for the special case of an orthogonal set of projectors on each site, the projection operator is self-adjoint and the above expressions reduce to the DFT+ U correction of Ref. 7.

Any set of localized functions may, in principle, be used as Hubbard projectors with which to define the occupancy matrix. Solutions of appropriate orbital symmetry of the hydrogenic Schrödinger equation, such as atomic-like or linear muffin-tin orbitals, are a common choice^{5,10,14}. These are generally characterized by an effective charge Z that determines their spatial diffuseness. For a given value of U , results of DFT+ U calculations with different values chosen for Z will not necessarily yield the same ground-state properties^{14,17}. Notwithstanding, hydrogenic orbitals may be inappropriate in cases in which the orbitals of the correlated manifold differ significantly from atomic wavefunctions.

In order to obtain accurate occupancies, a set of projectors is required which adequately accounts for electronic hybridization and which, if possible, is defined unambiguously for the system under study. Wannier functions, in particular maximally-localized Wannier functions (MLWFs)¹⁸, form just such an accurate minimal basis. They have been used with good effect to augment DFT with localized many-body interactions¹⁹, and there is numerical evidence to suggest that MLWFs constitute the projector set which maximizes the U parameter¹².

We work with the single-particle density-matrix, which is expressed in separable form²⁰ $\rho(\mathbf{r}, \mathbf{r}') =$

$\sum_{\alpha\beta} \phi_\alpha(\mathbf{r}) K^{\alpha\beta} \phi_\beta(\mathbf{r}')$ in terms of a localized basis of NGWFs²¹ $\{\phi_\alpha(\mathbf{r})\}$, related to the Kohn-Sham eigenstates by a linear transformation $\psi_n^{(\sigma)}(\mathbf{r}) = \sum_\alpha \phi_\alpha(\mathbf{r}) M_n^{(\sigma)\alpha}$. The density kernel $K^{\alpha\beta} = \langle \phi^\alpha | \hat{\rho} | \phi^\beta \rangle$ is the representation of the single-particle density operator $\hat{\rho}$ in terms of the contravariant duals $\{\phi^\alpha(\mathbf{r})\}$ of the NGWFs, which satisfy $\langle \phi_\alpha | \phi^\beta \rangle = \delta_\alpha^\beta$. The NGWFs are in turn expanded in terms of a systematic basis of Fourier-Lagrange, or psinc²², functions. The size of this basis is determined by an energy cutoff, akin to a plane-wave kinetic energy cutoff, with respect to which calculations are converged. The DFT energy functional is iteratively minimized with respect to both the density kernel and the NGWF expansion coefficients. The minimization scheme in the ONETEP linear-scaling code is detailed in Refs. 23.

These NGWFs, therefore, are a readily accessible set of localized orbitals which are calculated with linear-scaling computational cost. Similarly to MLWFs, NGWF centres may be used to calculate polarizabilities¹⁶. Thus, in this framework, it is natural to use a localised subset of Wannier functions obtained at the end of a ground-state calculation, with appropriate orbital character, as Hubbard projectors for defining the DFT+ U occupancy matrix. NGWFs are adapted to their chemical environment, reflecting the balance between the competing tendencies of electron itinerancy and localization in strongly correlated systems and, as a result, provide an accurate representation of the occupancy of the correlated site.

We propose a projector self-consistent scheme whereby the Hubbard projectors are determined self-consistently by iteratively solving for the Kohn-Sham ground-state using the Hubbard projectors defined by NGWFs from the DFT+ U ground-state energy calculation of the previous iteration. In this way, the Hubbard projectors converge to those that are optimally adapted for their own DFT+ U ground-state density. This scheme, as we go on to show, rapidly and monotonically converges to an unambiguously defined DFT+ U ground-state which, for a given U parameter, is of lowest energy. In other words, the DFT+ U energy functional is additionally minimized with respect to the set of localized NGWF projectors that are, at convergence, self-consistent with the DFT+ U calculation from which they are determined.

We applied our method to iron porphyrin (FeP). Metalloporphyrin systems, such as FeP, play an important role in biochemistry. The ability of metalloporphyrins to bind simple molecules is of interest, particularly in the case of FeP which can have a greater affinity for CO and NO than O₂, resulting in hindrance of respiration.

We performed fully converged energy minimization on FeP, and its complex with carbon monoxide, using the ONETEP code²³. We used spin-polarized DFT+ U within the generalized-gradient (GGA)²⁴ and pseudopotential²⁵ approximations. An equivalent plane-wave kinetic energy cutoff of 1000 eV was used with a cubic simulation cell of side-length 37 Å. The NGWFs were spatially restricted to atom-centered spheres of radius 5.3 Å and no density kernel truncation was applied. Since the

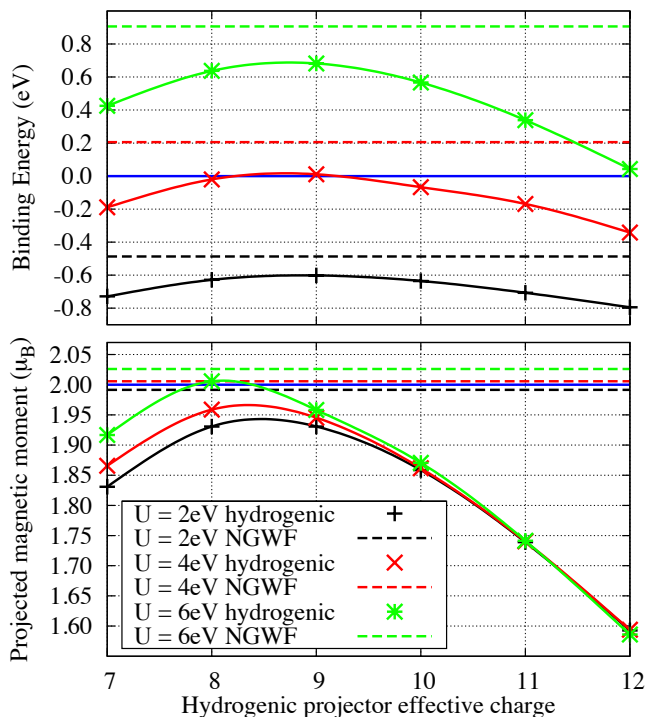


FIG. 1. (Color online) The interaction energy, positive for an unbound ligand, of the CO and FeP moieties (top panel) and the magnetic dipole moment projected onto the correlated manifold of triplet-state FeP (bottom panel). Both are plotted at various U as a function of the effective charge Z used to define the hydrogenic projectors (solid lines), while dashed lines show those quantities calculated with self-consistent NGWF Hubbard projectors. Blue lines indicate the binding threshold (top) and the ideal projected moment (bottom).

principal focus of this study was the dependence of computed DFT+ U ground-state properties on variations in the Hubbard projectors for a given U value, optimized PBE ($U = 0$ eV) structures were used.

Shown in Fig. 1, is the interaction energy between FeP and CO as an illustration that the binding affinity between moieties in DFT+ U can be strongly influenced by the localization of the Hubbard projectors. As can be seen, binding affinity is by no means uniquely defined when hydrogenic projectors are used, although this may be partly compensated by a projector-dependent first-principles^{7,14} U parameter. At $U = 6$ eV it varies from approximately 0.04 eV to 0.69 eV over the range of Z considered; at $U = 4$ eV the result is even qualitatively ambiguous as a function of Z . Using self-consistent NGWF projectors (dashed lines) generally results in energetically less favourable ligand binding, demonstrating that, for a given value of U , NGWF projectors more effectively counteract the spurious tendency of GGA functionals to over-bind ligands to FeP²⁶. Also shown in Fig. 1, the projected magnetic dipole moment of FeP in its ground-state varies strongly with the value of Z chosen for hydrogenic projectors (solid line), with only a narrow range of Z at

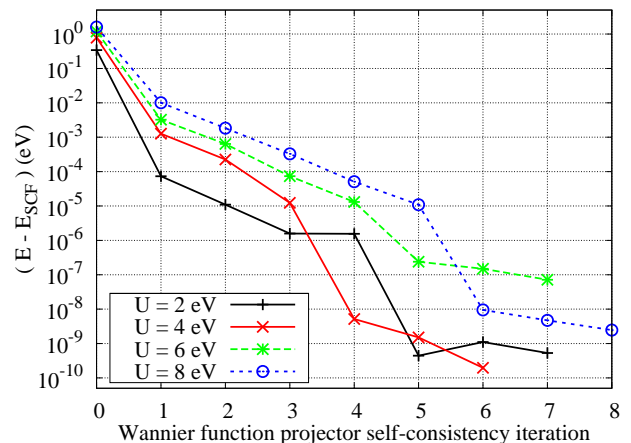


FIG. 2. (Color online) The difference in total energy E and the total energy at projector self-consistency E_{SCF} as a function of the projector self-consistency iteration. The procedure is initialized (iteration 0) with a set of hydrogenic $3d$ projectors to construct the correlated subspace, using the Clementi-Raimondi²⁷ effective charge of $Z = 11.17$ for iron $3d$ orbitals.

$U = 6$ eV giving values that are close to the expected $2.0 \mu_B$ for optimal projectors. Moreover, a pathological inconsistency with experiment emerges in that U values of sufficient magnitude to achieve the requisite moment (for some Z) bring us into the unphysical regime where FeP+CO binding is disfavoured. Conversely, the use of self-consistent NGWF projectors (dashed) results in a projected magnetic moment which lies within the physically reasonable range and is rather insensitive to U .

Fig. 2 demonstrates the stable convergence of the Hubbard projector self-consistency scheme for FeP+CO at different values of U . Each data point represents an individual variational total-energy minimization, wherein the Hubbard projectors are re-constructed from the optimized ground-state NGWFs from the previous iteration. The energy decreases rapidly as the projectors are refined, converging within a small number of iterations. This confirms our understanding that the Wannier are optimally adapted for the hybridized character of the electronic orbitals, while minimizing the energy. In this way, more spatially diffuse self-interaction corrections are introduced than with purely atomic orbitals, in a complimentary manner to such methods as DFT+ U + V ²⁸ which allow more general interaction terms between sites.

Since we re-use the self-consistent density from the previous projector iteration to initialise the following iteration, much fewer NGWF optimization steps are required at each successive projector update step. As demonstrated in Fig. 3, this results in an overall computational effort for achieving projector self-consistency that is only a small overhead compared to the conventional approach.

In order to achieve meaningful insight into the U -dependence of bond formation, it is necessary to allow for Hubbard projector update consistent with variations in the molecular geometry. We stress that ionic force

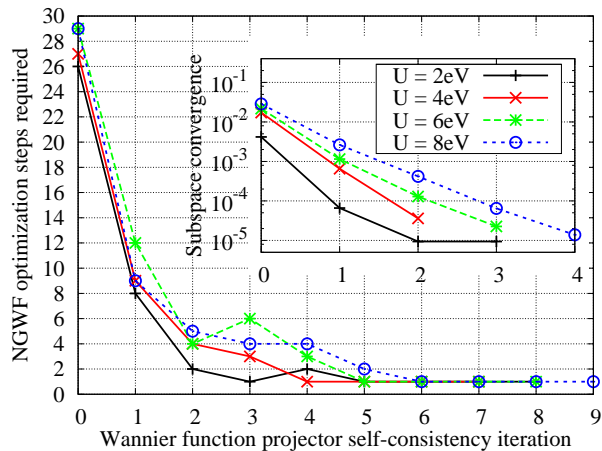


FIG. 3. (Color online) The number of NGWF optimization steps needed to converge the total energy for each projector self-consistency iteration for FeP+CO. Shown inset is the convergence of the correlated subspace, as quantified by its $3d$ -orbital character.

expressions are not complicated by the inclusion of self-consistent Hubbard projectors, with no additional terms appearing over those in conventional DFT+ U .

In conclusion, we have proposed and demonstrated a method within DFT+ U for obtaining Hubbard projectors that are uniquely-defined, optimally adapted to their chemical environment, and consistent with the DFT+ U ground-state density. Our implementation may be incorporated into any method that either solves directly for localized Wannier-like states, or which computes such states in a post-processing fashion. If combined self-consistently with approaches for calculating U from first-principles^{7,14}, this work opens up the possibility of parameter-free DFT+ U calculations on large systems.

ACKNOWLEDGMENTS

This research was supported by EPSRC, RCUK and the National University of Ireland. Calculations were performed on the Cambridge HPCS Darwin computer under EPSRC grant EP/F032773/1.

- * ddo20@cam.ac.uk
- ¹ J. S. Miller and A. J. Epstein, *Angew. Chem. Int. Ed. Engl.*, **33**, 385 (1994).
 - ² B. C. H. Steele and A. Heinzl, *Nature*, **414**, 345 (2001).
 - ³ R. H. Holm, P. Kennepohl, and E. I. Solomon, *Chem. Rev.*, **96**, 2239 (1996).
 - ⁴ P. Hohenberg and W. Kohn, *Phys. Rev.*, **136**, B864 (1964); W. Kohn and L. J. Sham, *ibid.*, **140**, A1133 (1965).
 - ⁵ K. Terakura, T. Oguchi, A. R. Williams, and J. Kübler, *Phys. Rev. B*, **30**, 4734 (1984); S. L. Dudarev, G. A. Botton, S. Y. Savrasov, C. J. Humphreys, and A. P. Sutton, *ibid.*, **57**, 1505 (1998).
 - ⁶ J. P. Perdew, R. G. Parr, M. Levy, and J. L. Balduz, *Phys. Rev. Lett.*, **49**, 1691 (1982).
 - ⁷ M. Cococcioni and S. de Gironcoli, *Phys. Rev. B*, **71**, 035105 (2005); H. J. Kulik, M. Cococcioni, D. A. Scherlis, and N. Marzari, *Phys. Rev. Lett.*, **97**, 103001 (2006).
 - ⁸ A. J. Cohen, P. Mori-Sanchez, and W. Yang, *Science*, **321**, 792 (2008).
 - ⁹ A. Svane and O. Gunnarsson, *Phys. Rev. Lett.*, **65**, 1148 (1990).
 - ¹⁰ V. I. Anisimov, J. Zaanen, and O. K. Andersen, *Phys. Rev. B*, **44**, 943 (1991); V. I. Anisimov, I. V. Solovyev, M. A. Korotin, M. T. Czyżyk, and G. A. Sawatzky, *ibid.*, **48**, 16929 (1993).
 - ¹¹ J. Hubbard, *Proc. R. Soc. London Ser. A*, **276**, 238 (1963); **277**, 237 (1964); **281**, 401 (1964).
 - ¹² T. Miyake and F. Aryasetiawan, *Phys. Rev. B*, **77**, 085122 (2008).
 - ¹³ A. A. Mostofi, J. R. Yates, Y.-S. Lee, I. Souza, D. Vanderbilt, N. Marzari, *Comp. Phys. Comm.*, **178**, 685 (2008).
 - ¹⁴ W. E. Pickett, S. C. Erwin, and E. C. Ethridge, *Phys. Rev. B*, **58**, 1201 (1998).
 - ¹⁵ M. J. Han, T. Ozaki, and J. Yu, *Phys. Rev. B*, **73**, 045110 (2006); K. K. H. Eschrig and I. Chaplygin, *Journal of Solid State Chemistry*, **176**, 482 (2003).
 - ¹⁶ Further details to appear in a forthcoming paper.
 - ¹⁷ S. Fabris, S. de Gironcoli, S. Baroni, G. Vicario, and G. Balducci, *Phys. Rev. B*, **72**, 237102 (2005).
 - ¹⁸ N. Marzari and D. Vanderbilt, *Phys. Rev. B*, **56**, 12847 (1997).
 - ¹⁹ F. Lechermann, A. Georges, A. Poteryaev, S. Biermann, M. Posternak, A. Yamasaki, and O. K. Andersen, *Phys. Rev. B*, **74**, 125120 (2006).
 - ²⁰ R. McWeeny, *Rev. Mod. Phys.*, **32**, 335 (1960).
 - ²¹ C.-K. Skylaris, A. A. Mostofi, P. D. Haynes, O. Diéguez, and M. C. Payne, *Phys. Rev. B*, **66**, 035119 (2002).
 - ²² A. A. Mostofi, P. D. Haynes, C.-K. Skylaris and M. C. Payne, *J. Chem. Phys.*, **119**, 8842 (2003); D. Baye and P.-H. Heenen, *J. Phys. A: Math. Gen.*, **19**, 2041 (1986).
 - ²³ C.-K. Skylaris, P. D. Haynes, A. A. Mostofi and M. C. Payne, *J. Chem. Phys.*, **122**, 084119 (2005); P. D. Haynes, C.-K. Skylaris, A. A. Mostofi, and M. C. Payne, *Chem. Phys. Lett.*, **422**, 345 (2006).
 - ²⁴ J. P. Perdew, K. Burke, and M. Ernzerhof, *Phys. Rev. Lett.*, **77**, 3865 (1996).
 - ²⁵ A. M. Rappe, K. M. Rabe, E. Kaxiras, and J. D. Joannopoulos, *Phys. Rev. B*, **41**, 1227 (1990); RRRJ Pseudopotentials were generated using the Opium code, <http://opium.sourceforge.net>, using the GGA input parameters available therein, albeit with a scalar-relativistic correction for all species and, for iron, a non-linear core correction of Fuchs-Scheffler characteristic radius 1.3a.u. and core-radius of 2.0a.u.
 - ²⁶ D. A. Scherlis, M. Cococcioni, P. Sit, N. Marzari, *J. Phys. Chem. B*, **111**, 7384 (2007).
 - ²⁷ E. Clementi and D. L. Raimondi, *J. Chem. Phys.*, **38**, 2686 (1963).
 - ²⁸ V. L. Campo Jr and M. Cococcioni, *Journal of Physics: Condensed Matter*, **22**, 055602 (2010).